Varying Coefficient Models for Modeling Diffusion Tensors Along White Matter Bundles

Ying Yuan, Hongtu Zhu, Steve Marron, John Gilmore, Martin Styner

Varying Coefficient Models for Modeling Diffusion Tensors Along White Matter Bundles

Ying Yuan[1], Hongtu Zhu[1], J. S. Marron[2], John H. Gilmore[3], and Martin Styner[4]

[1] Dept Biostatistics, UNC Chapel Hill
[2] Dept Operations Research and Statistics, UNC Chapel Hill
[3] Dept Psychiatry, UNC Chapel Hill
[4] Dept Psychiatry and Computer Science, UNC Chapel Hill

Abstract. This paper develops a functional data analysis framework to model diffusion tensors along fiber bundles as functional responses with a set of covariates of interest, such as age, diagnostic status and gender. This framework has a wide range of clinical applications including the characterization of normal brain development, the neural bases of neuropsychiatric disorders, and the joint effects of environmental and genetic factors on white matter fiber bundles. A challenging statistical issue is how to appropriately handle diffusion tensors along fiber bundles as functional data in a Riemannian manifold. We propose a statistical model with varying coefficient functions,called VCTF to characterize the dynamic association between functional SPD matrix-valued responses and covariates. We calculate a weighted least squares estimation of the varying coefficient functions under the Log-Euclidean metric in the space of SPD matrices. We also develop a global test statistic to test specific hypotheses about these coefficient functions. Simulated data are further used to examine the finite sample performance of VCTF . We apply our VCTF to study potential gender differences and find statistically significant aspect of the development of diffusion tensors along the right internal capsule tract in a clinical study of neurodevelopment.

1 Introduction

Diffusion Tensor Imaging (DTI), which can track the effective diffusion of water in the human brain *in vivo*, has been widely used to map the microstructure and organization of fiber tracts and to assess the integrity of anatomical connectivity in white matter [1]. In DTI, the degree of diffusivity and the directional dependence of water diffusion in each voxel can be quantified by a 3×3 symmetric positive definite (SPD) matrix, called a diffusion tensor (DT), and its three eigenvalue-eigenvector pairs $\{(\lambda_k, \mathbf{v}_k) : k = 1, 2, 3\}$ with $\lambda_1 \geq \lambda_2 \geq \lambda_3$. Fiber tracts in white matter can be constructed by consecutively connecting the principal directions ($\mathbf{v}_1$) of DTs in adjacent voxels [2]. Therefore, DTs and tensor-derived quantities (e.g., fractional anisotropy (FA)) are distributed along these white matter fiber tracts for each subject. As an illustration, Figure 1 (a)

presents the right internal capsule tract and Figure 1 (b) presents DTs along this tract obtained from 10 subject's, in which each DT is geometrically represented by an ellipsoid. In this representation, the lengths of the semiaxes of the ellipsoid equal the square root of the eigenvalues of a DT, while the eigenvectors define the direction of the three axes. Mathematically, these diffusion tensors along the fiber tract are functionals of SPD matrices. Our research of interest is to statistically model SPD functionals as responses with covariates of interest, such as age and gender, across multiple subjects.

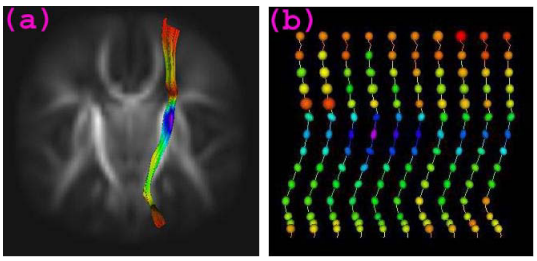

Fig. 1. (a) The right internal capsule tract. (b) The ellipsoidal representation of full tensors on the fiber tract from 10 selected subjects, colored with FA values.

Statistical approaches have been developed for the statistical analysis of tensor-derived quantities along fiber tracts. A tract-based spatial statistics framework was developed to construct local diffusion properties along a white matter skeleton and then perform pointwise hypothesis tests at each grid point of the skeleton [3]. A model-based framework was developed to construct the medial manifolds of fiber tracts and then to test pointwise hypotheses based on diffusion properties along the medial manifolds [4]. However, since these two methods ignore the functional nature of diffusion properties along fiber tracts, they can suffer from low statistical power in detecting interesting features and in exploring variability in tract-based diffusion properties. A functional data analysis framework was used to compare a univariate diffusion property along fiber tracts across two (or more) populations for a single hypothesis test per tract by using functional principal component analysis and the Hotelling T^2 statistic [5]. Their method has two major limitations including only consideration of a univariate diffusion property and the lack of control for other covariates of interest, such as age. To address these two limitations, a functional regression framework was proposed to analyze multiple diffusion properties along fiber tracts as functional responses with a set of covariates of interest, such as age, diagnostic status and gender [6]. An alternative approach, called generalized functional linear models, was developed with a scalar outcome (e.g., diagnostic group) as responses and fiber bundle diffusion properties as varying covariate functions (or functional predictors) [7].

The calculated diffusion properties, which are nonlinear and linear functions of the estimated three eigenvalues of DT containing inherent bias, may be substantially different from the true diffusion properties [8]. Numerical simulations have shown that estimates of the largest eigenvalue in a DT usually overestimate the true value of λ_1 and that estimates of the smallest eigenvalue usually underestimate λ_3. These differences between the estimated and true eigenvalues subsequently bias the estimation of diffusion properties that are calculated from the values of these estimated eigenvalues. The sorting bias is pronounced in three types of degenerate DT including isotropic ($\lambda_1 = \lambda_2 = \lambda_3$), oblate ($\lambda_1 = \lambda_2 > \lambda_3$), or prolate ($\lambda_1 > \lambda_2 = \lambda_3$). Previous studies have shown that a major portion of DTs along fiber tracts are prolate tensors [9], and thus directly comparing these biased diffusion properties along fiber tracts can create 'statistical artifacts' including biased parameter estimates and incorrect test statistics and $p-$values for hypotheses of interest as shown in Section 3.

To avoid these statistical artifacts, it is important to directly analyze estimated DTs along fiber tracts. There are several advantages of comparing the estimated DTs along fiber tracts with covariates. The first one is that the standard weighted least squared estimates of true DTs are almost unbiased [8]. Moreover, as shown in Section 3, directly modeling DTs along fiber tracts as a smooth SPD process allows us to incorporate smoothness constraint to further reduce noise in the estimated DTs along fiber tracts, which subsequently leads to reduced noise in estimated diffusion properties along the fiber tracts. Furthermore, the use of scalar diffusion properties ignores the direction information of DT, and thus it can lose the statistical power in detecting the differences in DT oriented in different directions.

There is a growing interest in the DTI literature in developing statistical methods for direct analysis of DTs in the space of SPD matrices. [10] proposed several parametric models for SPD matrices and derived the distributions of several test statistics for comparing differences between the means of the two (or multiple) groups of SPD matrices. [11] developed a nonparametric estimator for the common density function of a random sample of positive definite matrices. [12] developed a semi-parametric regression model with SPD matrices as responses in a Riemannian manifold and covariates in a Euclidean space. [13] and [14] proposed tensor splines and local constant regressions for interpolating DTI tensor fields based on the Riemannian metric.

In this paper, we propose a varying coefficient model (VCTF) to use varying coefficient functions to characterize the association between fiber bundle diffusion tensors and a set of covariates. This model is different from that in [12] because the former is applicable to DT-valued functional data and consider the within-subject correlations while the latter is only applicable to data with a DT response for each subject. Since the space of SPD matrices is a Riemanian manifold, to the best of our knowledge, our VCTF is the first paper for developing a functional data analysis framework for modeling functional manifold-valued responses with covariates in Euclidean space. To account for the curved nature of the SPD space, we employ the Log-Euclidean metric in [15] and then

use a weighted least squares estimation method based on the geodesic distance under the Log-Euclidean metric to estimate the varying coefficient functions. Furthermore, we develop global test statistics to test hypotheses on the varying coefficient functions and use a resampling method for approximating its p-value.

The rest of the paper is organized as follows. Section 2 presents VCTF and related statistical inference. Section 3 examines the finite sample performance of VCTF via simulation studies. Section 4 illustrates an application of VCTF in a clinical study of neurodevelopment. Section 5 presents concluding remarks.

2 Methodologies

In this section, we present our VCTF for the statistical analysis of DTs along fiber tracts as functional responses with a set of covariates. To compare DTs in populations of DTIs, we use the DTI atlas building followed by atlas fiber tractography and fiber parametrization as described in [5] to extract DTI fibers and establish DTI fiber correspondence across all DTI fiber correspondence across all DTI datasets from different subjects. For the sake of simplicity, we do not include these image processing steps here, which have been discussed in details in [5].

Varying Coefficient Model for Functional SPD data Let $\mathrm{Sym}^+(3)$ and $\mathrm{Sym}(3)$ be, respectively, the set of 3×3 SPD matrices and the set of 3×3 symmetric matrices with real entries. Let $\mathrm{vecs}(C) = (c_{1,1}, c_{2,1}, c_{2,2} \cdots, c_{m_1,1}, \cdots, c_{m_1,m_1})^T$ for any $m_1 \times m_1$ symmetric matrix $C = (c_{k,l})$. Let $\mathrm{Ivecs}(\cdot)$ be the inverse operator of $\mathrm{vecs}(\cdot)$ and (a_l) be a $q \times 1$ vector with the l-th element a_l. Let $C \otimes D$ denote the Kronecker product of two matrices C and D.

Let $x \in [0, L_0]$ be the arc length of any point on a specific fiber bundle relative to a fixed end point of the fiber bundle, where L_0 is the longest arc length on the fiber bundle. For the i-th subject, we measure a diffusion tensor, denoted by $S_i(x_j) \in \mathrm{Sym}^+(3)$, at the arc length $x_j \in [0, L_0]$ for the j-th location grid point on the fiber bundle for $j = 1, \cdots, n_G$ and $i = 1, \cdots, n$, where n_G and n denote the numbers of grid points and subjects, respectively. We consider a varying coefficient model given as follows:

$$\log(S_i(x)) = \mathrm{Ivecs}((\mathbf{z}_i^T \beta_l(x))) + \mathcal{U}_i(x) + \mathcal{E}_i(x) \quad \text{for} \quad i = 1, \cdots, n, \tag{1}$$

where $\log(\cdot)$ denotes the matrix logarithm, $\mathcal{E}_i(x) \in \mathrm{Sym}(3)$ is a 3×3 symmetric matrix of measurement errors, and $\mathcal{U}_i(x) \in \mathrm{Sym}(3)$ characterizes both individual matrix variations from $\mathrm{Ivecs}((\mathbf{z}_i^T \beta_l(x)))$ and the correlation structure between $\log(S_i(x))$ and $\log(S_i(x'))$ for different x and x'. Moreover, $\mathbf{z}_i$ and $\beta_l(x) = (\beta_{1l}(x), \cdots, \beta_{rl}(x))^T$ are, respectively, a $r \times 1$ vector of covariates of interest with $z_{i,1} = 1$ and its associated vector of varying coefficient functions of x for $l = 1, \cdots, 6$. Model (1) can be regarded as a generalization of varying coefficient models, which have been widely studied and developed for longitudinal, time series, and functional data.

Let $\mathrm{SP}(\mu, \Sigma)$ denote a stochastic process with mean $\mu(x)$ and covariance matrix function $\Sigma(x, x')$ for any $x, x' \in [0, L_0]$. It is also assumed that $\mathrm{vecs}(\mathcal{E}_i(x))$ and $\mathrm{vecs}(\mathcal{U}_i(x))$ are independent and respectively, independent and identical copies of $SP(\mathbf{0}, \Sigma_{\mathcal{E}})$ and $SP(\mathbf{0}, \Sigma_{\mathcal{U}})$. Moreover, $\mathrm{vecs}(\mathcal{E}_i(x))$ and $\mathrm{vecs}(\mathcal{E}_i(x'))$ for $x \neq x'$ are assumed to be independent and thus $\Sigma_{\mathcal{E}}(x, x')$ takes the form of $\Sigma_{\mathcal{E}}(x)\mathbf{1}_{x=x'}$.

Weighted Least Squares Estimation To estimate the coefficient functions in $\beta(x) = (\beta_1^T(x), \cdots, \beta_q^T(x))^T$, we develop a weighted least squares estimation method based on an adaptive local polynomial kernel (LPK) smoothing technique [16] and the geodesic distance under the Log-Euclidean metric (see [15] for details). Specifically, using Taylor's expansion, we can expand $\beta_l(x_j)$ at x to obtain $\beta_l(x_j) \approx \beta_l(x) + \dot{\beta}_l(x)(x_j - x)$,

For a fixed bandwidth $h^{(1)}$, we first calculate a weighted least squares estimate of $\beta_l(x)$, denoted by $\hat{\beta}_l(x)$, which minimizes an objective function given by $\sum_{i=1}^{n}\sum_{j=1}^{n_G} K_{h^{(1)}}(x_j - x)\mathrm{tr}\{[\log(S_i(x_j)) - \mathrm{Ivecs}((\mathbf{z}_i^T(\beta_l(x) + \dot{\beta}_l(x)(x_j - x))))]^{\otimes 2}\}$, where $K_{h^{(1)}}(\cdot) = K(\cdot/h^{(1)})/h^{(1)}$ is a rescaled kernel function, $K(\cdot)$ be a kernel function, such as the Gaussian and uniform kernels [16] and $\mathbf{a}^{\otimes 2} = \mathbf{a}\mathbf{a}^T$ for any vector or any matrix $\mathbf{a}$. Then with some calculation, we can have

$$\hat{\beta}_l(x) = (\hat{\beta}_{1k}(x), \cdots, \hat{\beta}_{rl}(x))^T = [I_r \otimes (1, 0)]A_l(x)), \tag{2}$$

where I_r is an $r \times r$ identity matrix, $A_l(x)) = \Sigma(h^{(1)}, x)^{-1}\sum_{i=1}^{n}\sum_{j=1}^{n_G} K_{h^{(1)}}(x_j - x)[\mathbf{z}_i \otimes \mathbf{y}_{h^{(1)}}(x_j - x)](\log(S_i(x_j)))_l$ and $\Sigma(h^{(1)}, x) = \sum_{i=1}^{n}\sum_{j=1}^{n_G} K_{h^{(1)}}(x_j - x)[\mathbf{z}_i^{\otimes 2} \otimes \mathbf{y}_{h^{(1)}}(x_j - x)^{\otimes 2}]$ with $\mathbf{y}_{h^{(1)}}(x_j - x) = (1, (x_j - x)/h^{(1)})^T$.

We pool the data from all n subjects and select an estimated bandwidth $h^{(1)}$, denoted by $\hat{h}_e^{(1)}$ by minimizing the cross-validation score given by $(nn_G)^{-1}\sum_{i=1}^{n}$ $\sum_{j=1}^{n_G}\mathrm{tr}\{[\log(S_i(x_j)) - \mathrm{Ivecs}((\mathbf{z}_i^T\hat{\beta}_l(x_j, h^{(1)})^{(-i)}))]^{\otimes 2}\}$, where $\hat{\beta}_l(x, h^{(1)})^{(-i)}$ is the weighted least squares estimator of $\beta_l(x)$ for the bandwidth $h^{(1)}$ based on observed data with the observations from the i-th subject excluded. Finally, by substituting $\hat{h}_e^{(1)}$ into (2), we can obtain an estimate of $\beta_l(x)$, denoted by $\hat{\beta}_{l,e}(x)$. Combining all $\hat{\beta}_{l,e}(x)$ leads to $\hat{\beta}_e(x) = [\hat{\beta}_{1,e}(x), \cdots, \hat{\beta}_{q,e}(x)]$.

Smoothing Individual Functions and Estimating Covariance Matrices To simultaneously construct the individual function $\mathcal{U}_i(x)$, we also employ the local polynomial kernel smoothing technique. Specifically, using Taylor's expansion, we can expand $\mathcal{U}_i(x_j)$ at x to obtain $\mathcal{U}_i(x_j) \approx \mathcal{U}_i(x) + \dot{\mathcal{U}}_i(x)(x_j - x)$. For each fixed x and each bandwidth $h^{(2)}$, we calculate the weighted least square estimator of $\mathcal{U}_i(x)$, denoted as $\hat{\mathcal{U}}_i(x)$, by minimizing an objective function given by $\sum_{j=1}^{n_G} K_{h^{(2)}}(x_j - \mathbf{x})\mathrm{tr}\{[\log(S_i(x_j)) - \mathrm{Ivecs}((\mathbf{z}_i^T\hat{\beta}_{l,e}(x_j))) - \mathcal{U}_i(x) + \dot{\mathcal{U}}_i(x)(x_j - x)]^{\otimes 2}\}$. With some calculation, it can be shown that the weighted least square estimate of $\mathcal{U}_i(x)$, denoted by $\hat{\mathcal{U}}_i(x)$, given by

$$\mathrm{vecs}(\hat{\mathcal{U}}_i(x))^T = \sum_{j=1}^{n_G} \tilde{K}_{h^{(2)}}^0(x_j - x, x)(\mathrm{vecs}(\log(S_i(x_j))) - (\mathbf{z}_i^T\hat{\beta}_{l,e}(x_j)))^T, \tag{3}$$

where $\tilde{K}^0_{h^{(2)}}(x_j - x, x) = \Sigma_1(h^{(2)}, x)^{-1} K_{h^{(2)}}(x_j - x)\mathbf{y}_{h^{(2)}}(x_j - x)$ is the empirical equivalent kernel and $\Sigma_1(h^{(2)}, x) = \sum_{j=1}^{n_G} K_{h^{(2)}}(x_j - x)\mathbf{y}_{h^{(2)}}(x_j - x)^{\otimes 2}$ with $\mathbf{y}_{h^{(2)}}(x_j - x) = (1, (x_j - x)/h^{(2)})^T$

Let R_i be a matrix with the j-th row $\text{vecs}(\log(S_i(x_j))) - (\mathbf{z}_i^T \hat{\beta}_{l,e}(x_j))^T$ and $\mathcal{S}$ be a $n_G \times n_G$ smoothing matrix with the (i,j)-th element $\tilde{K}^0_{h^{(2)}}(x_j - x_i, x_i)$. We pool the data from all n subjects and select an estimated bandwidth of $h^{(2)}$, denoted as $\hat{h}_e^{(2)}$, by minimizing the generalized cross-validation score given by $n^{-1} \frac{\sum_{i=1}^n \text{tr}\{(R_i - \mathcal{S}R_i)^{\otimes 2}\}}{(1 - n^{-1}\text{tr}(\mathcal{S}))^2}$. Based on $\hat{h}_e^{(2)}$, we can use (3) to estimate $\text{vecs}(\mathcal{U}_i(x))$ and $\mathcal{U}_i(x)$, denoted by $\text{vecs}(\hat{\mathcal{U}}_{i,e}(x))$ and $\hat{\mathcal{U}}_{i,e}(x)$, respectively, for all i. After obtaining $\hat{\mathcal{U}}_{i,e}(x)$, we can estimate the mean function $\mathcal{U}(x)$ and the covariance function $\Sigma_{\mathcal{U}}(x, x')$ by using their empirical counterparts.

We construct a nonparametric estimator of the covariance matrix $\Sigma_{\mathcal{E}}(x, x)$ as follows. Let $\hat{\mathcal{E}}_i(x_j) = \log(S_i(x_j)) - \text{Ivecs}((\mathbf{z}_i^T \hat{\beta}_{l,e}(x_j))) - \hat{\mathcal{U}}_{i,e}(x_j)$ be estimated residuals for $i = 1, \cdots, n$ and $j = 1, \cdots, n_G$. We consider the kernel estimate of $\Sigma_{\mathcal{E}}(x, x)$ given by

$$\hat{\Sigma}_{\mathcal{E}}(x, x) = (n - q)^{-1} \sum_{i=1}^{n} \sum_{j=1}^{n_G} \frac{K_{h^{(3)}}(x_j - x)\text{vecs}(\hat{\mathcal{E}}_i(x_j))^{\otimes 2}}{\sum_{j=1}^{n_G} K_{h^{(3)}}(x_j - x)}. \tag{4}$$

Let $\tilde{\Sigma}_{\mathcal{E}}(x_j, x_j) = (n - q)^{-1} \sum_{i=1}^n \text{vecs}(\hat{\mathcal{E}}_i(x_j))^{\otimes 2}$. To select an estimated bandwidth $h^{(3)}$, denoted by $\hat{h}_e^{(3)}$, we minimize the cross-validation score given by $(nn_G)^{-1} \sum_{i=1}^n \sum_{j=1}^{n_G} \text{tr}\{[\text{vecs}(\hat{\mathcal{E}}_i(x_j))^{\otimes 2} - \hat{\Sigma}_{\mathcal{E}}(x_j, x_j, h^{(3)})^{(-i)}]^{\otimes 2} \tilde{\Sigma}_{\mathcal{E}}(x_j, x_j)^{-1}]^{\otimes 2}\}$, where $\hat{\Sigma}_{\mathcal{E}}(x, x, h^{(3)})^{(-i)}$ is the weighted least squares estimator of $\hat{\Sigma}_{\mathcal{E}}(x, x)$ based on observed data with the observations from the i-th subject excluded. Based on $\hat{h}_e^{(3)}$, we can use (4) to estimate $\Sigma_{\mathcal{E}}(x, x)$, denoted by $\hat{\Sigma}_{\mathcal{E},e}(x, x)$.

Hypothesis Test In neuroimaging studies, some scientific questions require the comparison of fiber bundle diffusion tensors along fiber bundles across two (or more) diagnostic groups and the assessment of the development of fiber bundle diffusion properties along time. Such questions can often be formulated as linear hypotheses of $\beta(x)$ as follows:

$$H_0 : \mathbf{R}\beta(x) = \mathbf{b}_0(x) \text{ for all } x \text{ vs. } H_1 : \mathbf{R}\beta(x) \neq \mathbf{b}_0(x), \tag{5}$$

where $\mathbf{R}$ is a $t \times 6r$ matrix of full row rank and $\mathbf{b}_0(x)$ is a given $t \times 1$ vector of functions .

We propose both local and global test statistics. The local test statistic can identify the exact location of significant grid point on a specific tract. At a given grid point x_j on a specific tract, we test the local null hypothesis $H_0(x_j) : \mathbf{R}\beta(x_j) = \mathbf{b}_0(x_j)$ against $H_1(x_j) : \mathbf{R}\beta(x_j) \neq \mathbf{b}_0(x_j)$. We use a local test statistic $T_n(x_j)$ defined by

$$T_n(x_j) = n\mathbf{d}(x_j)^T \{\mathbf{R}(\hat{\Sigma}_{\mathcal{U}}(x_j, x_j) \otimes \hat{\Omega}_Z^{-1})\mathbf{R}^T\}^{-1}\mathbf{d}(x_j), \tag{6}$$

where $\hat{\Omega}_Z = n^{-1}\sum_{i=1}^{n}\mathbf{z}_i^{\otimes 2}$ and $\mathbf{d}(x) = \mathbf{R}(\hat{\beta}_o(x)^T - \text{bias}(\hat{\beta}_o(x)^T)) - \mathbf{b}_0(x)$. Following [17], a smaller bandwidth leads to a small value of bias$(\hat{\beta}_o(x))$. Moreover, according to our simulation studies below, we have found that the effect of dropping bias$(\hat{\beta}_o(x))$ is negligible and therefore, we drop it from now on.

We test the null hypothesis $H_0 : \mathbf{R}\beta(x) = \mathbf{b}_0(x)$ for all x using a global test statistic T_n defined by

$$T_n = n\int_0^{L_0} \mathbf{d}(x)^T[\mathbf{R}(\hat{\Sigma}_{\mathcal{U}}(x,x)\otimes\hat{\Omega}_X^{-1})\mathbf{R}^T]^{-1}\mathbf{d}(x)dx. \tag{7}$$

It follows from Theorem 1 [18] along with the continuous mapping theorem that as both n and n_G converges to infinity, we have T_n converges to some distribution (weighted χ^2). Based on this result, we develop a wild bootstrap method to approximate the p-value of T_n.

3 Simulation Studies

We conducted two sets of Monte Carlo simulations. The first set of simulations was to evaluate the Type I and II error rates of the global test statistic T_n. The second set was to compare the power in detecting the group effect using either whole diffusion tensor or the diffusion properties.

Simulation 1 In the first set of simulations, we evaluated the Type I and II error rates by simulating diffusion tensors along the right internal capsule tract (Figure 1 (a)) according to $S_i(x) = \exp(\text{Ivecs}((\beta_{1l}(x) + \beta_{2l}(x)\times \text{G}_i + \beta_{3l}(x)\times \text{Gage}_i)) + \mathcal{U}_i(x) + \mathcal{E}_i(x))$, where Gage_i and G_i, respectively, denote the gestational age at the scan time and gender of the i-th infant, vecs$(\mathcal{U}_i(x))$ is a Gaussian process with zero mean and covariance matrix $\Sigma_{\mathcal{U}}(x,x')$ and vecs$(\mathcal{E}_i(x))$ is a Gaussian random vector with zero mean and covariance matrix $\Sigma_{\mathcal{E}}(x,x)\mathbf{1}(x = x')$. To mimic imaging data, we used the diffusion tensors along the right internal capsule tract from all the 96 infants in our clinical data to estimate $\hat{\beta}(x)$ of $\beta(x)$ via equation (2), $\hat{\mathcal{U}}(x)$ of $\mathcal{U}(x)$ via equation (3), and $\hat{\mathcal{E}}(x)$ of $\mathcal{E}(x)$ via $\hat{\mathcal{E}}(x) = \log(S_i(x)) - \text{Ivecs}((\hat{\beta}_l(x)^T\mathbf{z})) - \hat{\mathcal{U}}(x)$. We fixed all the parameters at their values obtained from our clinical data, except that we assumed $(\beta_{31}(x),\cdots,\beta_{36}(x)) = c(\hat{\beta}_{31}(x),\cdots,\hat{\beta}_{36}(x))$, where c is a scalar specified below and $(\hat{\beta}_{31}(x),\cdots,\hat{\beta}_{36}(x))$ were estimators obtained from our clinical data. Figure 2 displays the estimated diffusion tensors using VCTF method when $c = 1$. Note that the method did an excellent job of recovering ground truth.

In neuroimaging studies, some scientific questions require the assessment of the development of fiber bundles diffusion tensors across time. In this simulation study, the questions were formulated as the hypotheses test $H_0 : \beta_{31}(x) = \cdots = \beta_{36}(x) = 0$ for all x along the right internal capsule tract against $H_1 : \beta_{3l}(x) \neq 0$ for at least one x on the tract for some $l = 1,\cdots,6$. We first assumed $c = 0$ to assess the Type I error rates for the global test statistic T_n, and then we assumed $c = .2, .4, .6$, and $.8$ to examine the Type II error rates for T_n at different effect

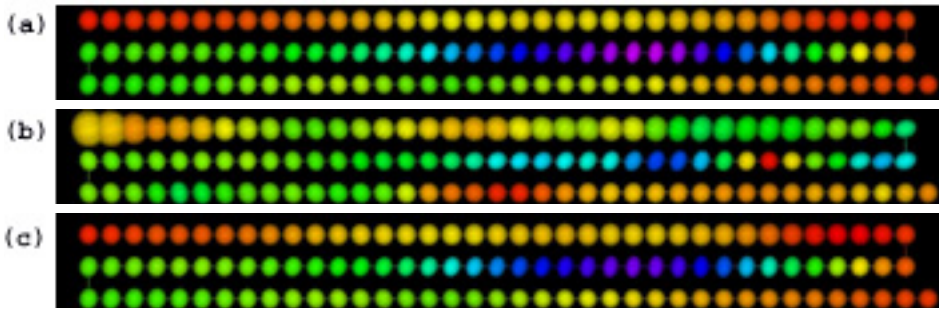

Fig. 2. Ellipsoidal representations of the true (a), simulated (b) and estimated (c) diffusion tensors along the the right internal capsule tract, colored with FA values.

sizes. To evaluate the Type I and II error rates at different sample sizes, we let $n = 96$. The values of gender and gestational age were set the same as all the 96 infants in our clinical study. Note that the number of grid points on the right internal capsule equals $n_G = 112$ for both cases.

We applied the VCTF procedure to the simulated diffusion tensors. Particularly, we approximated the p-value of T_n using the wild bootstrap method described in the hypothesis test section. For each simulation, the significance levels were set at $\alpha = .05$ and .01, and 100 replications were used to estimate the rejection rates. For a fixed α, if the Type I rejection rate is smaller than α, then the test is conservative, whereas if the Type I rejection rate is greater than α, then the test is anticonservative, or liberal.

Figure 3(a) displays the rejection rates for T_n based on the resampling method for sample size 96) and all effect sizes ($c = 0, .2, .4, .6,$ or $.8$) at both significance levels ($\alpha = .01$ or $.05$) using full diffusion tensors. The statistical power for rejecting the null hypothesis increases with the effect size and the significance level, which is consistent with our expectation.

Simulation 2 In the second set of simulations, the diffusion tensors along the fiber tract were generated as in the first set of simulation. For each simulated diffusion tensor, we calculated its FA and MD values. Then we applied the VCTF procedure for multiple measures to the simulated values of FA, MD, joint FA and MD, respectively, and then tested the significance of the gestational age effect. It is observed from Fig. 3 (a)-(c) that the statistical power is much higher when we use the whole tensor instead of FA and MD. The power is a little higher at small effect size when we use the joint FA and MD values instead of full diffusion tensors while at higher effect size, they almost have the same power (Fig. 3(a) and (d)). However, the Type I error is greater than the .05 significance level when we use the joint FA and MD values (Fig. 3(d)). It means that the test is liberal. As mentioned in Section 1, this is because there is some inherent bias in these calculated diffusion properties.

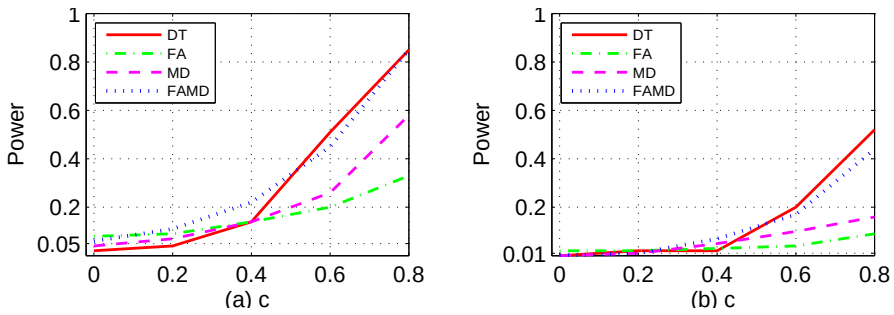

Fig. 3. Simulation study: Type I and Type II error rates. Rejection rates of $\mathbf{T}_n$ based on the resampling method are calculated at five different values of c for sample sizes of 96(solid lines) subjects at the (a) .05 and (b) .01 significance levels using diffusion tensor, FA values, MD values, joint values of FA and MD.

4 A Real Example

We investigate early brain development by using DTI and our VCTF. We consider 96 healthy infants (36 males and 60 females) whose mean gestational age was 245.6 days with SD: 18.5 days (range: 192-270 days). A 3T Allegra head only MR system was used to acquire all the images. The system was equipped with a maximal gradient strength of 40 mT/m and a maximal slew rate of 400 mT/(m·msec). The DTI images were obtained by using a single shot EPI DTI sequence (TR/TE=5400/73 msec) with eddy current compensation. The six non-collinear directions at the b-value of 1000 s/mm^2 with a reference scan (b=0) was applied. To improve the signal-to-noise ratio of the images, a total of five scans were acquired and averaged. A weighted least square estimation method [1] was used to construct the diffusion tensors. Then DTI atlas building followed by atlas based tractography procedure was employed to process all 96 DTI datasets. A nonlinear fluid deformation based highdimensional, unbiased atlas computation method is used to carry out a large deformation non-linear registration [19]. We chose the right internal capsule tract to illustrate the applicability of our method. Diffusion tensors were extracted along this fiber tract for all the 96 infants [5].

In this study, we have two specific aims. The first one is to compare diffusion tensors along the selected fiber bundle across the male and female groups and thus illuminate the gender effect on the development of these fiber bundle diffusion tensors. The second one is to delineate the development of fiber bundle diffusion tensor across the gestational age effect. To statistically test the effects, we applied our VCTF to diffusion tensors along the fiber tract. For the selected tract, we fitted the VCTF model (1) to the diffusion tensors from all 96 subjects, in which $\mathbf{z} = (1, \text{gender}, \text{Gage})^T$. Then, we used equation (2) to estimate the functional coefficients $\beta(x)$. For the hypothesis testing, we constructed the global test statistic T_n via equation (7) to test the gender and age effects for the diffusion tensors. The p value of T_n was approximated using the resampling

method with $G = 1,0000$ replications. Furthermore, we fitted VCTF model to FA, MD,joint FA and MD, each of three eigenvalues and three eigenvalues together values along the fiber tract.

In this study, we statistically test the effects of gender and gestational age on the diffusion tensors along the right internal capsule tract. To test the gender effect, we calculated the local test statistics $T_n(x_j)$ and their corresponding p values across all grid points on the right internal capsule tract. It is observed from Figure 4 (a) that most grid points do not have significant $-\log_{10}(p)$ values, which are less than 1.3. Then, we also computed the p-value of the global test statistic $\mathbf{T}_n$, $p = .335$ indicating no gender effect. It is observed from Figure 4 (b) that the $-\log_{10}(p)$ values of $T_n(x_j)$ for testing the gestational age effect at some grid points of the right tail are greater than 1.5 while a very high significant gestational age effect was found with the $p-$ value of the global test statistic, $p = .01$. This indicates that diffusion tensors along the right internal capsule tract do not differ significantly between male and female groups but are significantly associated with the gestational age.We picked a grid point with the significant p value of $T_n(x)$ and observed that the diffusion tensors become more spherical with the gestational age (Figure 5). This indicates a decreasing pattern of diffusion.

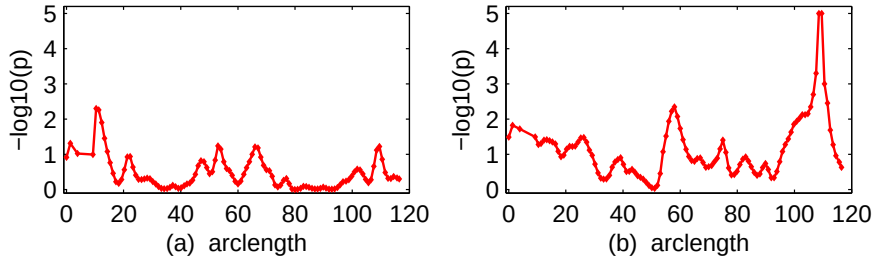

Fig. 4. The $-\log_{10}(p)$ values of test statistics $T_n(x_j)$ for testing gender (a) or gestational age (b) effect of diffusion tensors on the right internal capsule tract.

5 Discussion

We have developed VCTF methods for diffusion tensors along fiber tracts in the Riemannian manifold of SPD matrices under the log-Euclidean metric. From the application end, VCTF is demonstrated in a clinical study of neurodevelopment for revealing the complex inhomogeneous spatiotemporal maturation patterns as the apparent changes in fiber bundle diffusion tensors. We have shown that this novel statistical tool leads to new findings in our clinical applications.

Another commonly used metric on the Riemannian manifold of SPD matrices is the Riemannian metric. In contrast, some operations, e.g. average or interpolation of a set of tensors under the Log-Euclidean and Riemannian metrics, are

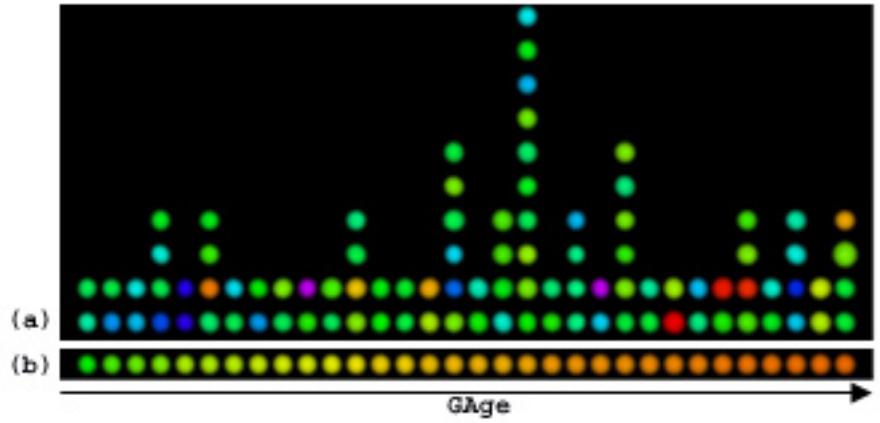

Fig. 5. The ellipsoidal representations of (a) Raw diffusion tensor of all 96 infants and (b) smoothed diffusion tensors changing with the gestational age at one point on the right internal capsule tract with significant gestational age effect.

theoretically and practically very similar [15]. Moreover, some statistical methods based on the two metrics have very similar results. However, the Riemannian metric is affine invariant. Affine invariance is a desirable feature for imaging processing, e.g. segmentation. In this scenario, as shown in [13], the method using the Riemannian metric outperformed the method using the Log-Euclidean metric. So it is interesting to develop VCTF under the Riemannian metric and then compare the statistical powers of detecting group differences under these two different metrics.

References

1. P. J. Basser, J. Mattiello, and D. LeBihan. Estimation of the effective self- diffusion tensor from the nmr spin echo. *Journal of Magnetic Resonance Ser. B*, 103:247–254, 1994.
2. P. J. Basser, S. Pajevic, C. Pierpaoli, J. Duda, and A. Aldroubi. In vivo fiber tractography using dt-mri data. *Magnetic Resonance in Medicine*, 44:625–632, 2000.
3. S. M. Smith, Jenkinson M., H. Johansen-Berg, D. Rueckert, T. E. Nichols, C. E. Mackay, K. E. Watkins, O. Ciccarelli, M.Z. Cader, P.M. Matthews, and T. E. Behrens. Tract-based spatial statistics: voxelwise analysis of multi-subject diffusion data. *NeuroImage*, 31:1487–1505, 2006.
4. P. A. Yushkevich, H. Zhang, T.J. Simon, and J. C. Gee. Structure-specific statistical mapping of white matter tracts. *Neuroimage*, 41:448–461, 2008.
5. C. B. Goodlett, P. T. Fletcher, J. H. Gilmore, and G. Gerig. Group analysis of dti fiber tract statistics with application to neurodevelopment. *NeuroImage*, 45:S133–S142, 2009.
6. H. T. Zhu, M. Styner, N. S. Tang, Z. X. Liu, W. L. Lin, and J.H. Gilmore. Frats: Functional regression analysis of dti tract statistics. *IEEE Transactions on Medical Imaging*, 29:1039–1049, 2010.

7. J. Goldsmith, J. Feder, C. M. Crainiceanu, B. Caffo, and D. Reich. Penalized functional regression. Technical report, Working Paper 2010-204, Johns Hopkins University Dept. of Biostatistics., 2010.
8. H. T. Zhu, H. P. Zhang, J. G. Ibrahim, and B. G. Peterson. Statistical analysis of diffusion tensors in diffusion-weighted magnetic resonance image data (with discussion). *Journal of the American Statistical Association*, 102:1085–1102, 2007.
9. H. T. Zhu, D. Xu, R. Amir, X. Hao, H. Zhang, K. Alayar, B. Ravi, and B. Peterson. A statistical framework for the classification of tensor morphologies in diffusion tensor images. *Magnetic Resonance Imaging*, 24:569–582, 2006.
10. A. Schwartzman, W. Mascarenhas, and J. E. Taylor. Inference for eigenvalues and eigenvectors of gaussian symmetric matrices. *Ann. Statist.*, 36:1423–1431, 2008.
11. P. T. Kim and D. S. Richards. *Deconvolution density estimation on spaces of positive definite symmetric matrices.* IMS Lecture Notes Monograph Series. A Festschrift of Tom Hettmansperger, 2010.
12. H. T. Zhu, Y. S. Cheng, J. G. Ibrahim, Y. M. Li, C. Hall, and W. L. Lin. Intrinsic regression models for positive definitive matrices with applications in diffusion tensor images. *Journal of the American Statistical Association*, 104:1203–1212, 2009.
13. A. Barmpoutis, B. C. Vemuri, T. M. Shepherd, and J. R. Forder. Tensor splines for interpolation and approximation of dt-mri with applications to segmentation of isolated rat hippocampi. *IEEE Transactions on Medical Imaging*, 26:1537–1546, 2007.
14. B. C. Davis, E. Bullitt, P. T. Fletcher, and S. Joshi. Population shape regression from random design data. *IEEE 11th International Conference on Computer Vision*, pages 1–7, 2007.
15. V. Arsigny. Processing data in lie groups: An algebraic approach. application to non-linear registration and diffusion tensor mri. Ph.D. dissertation, 2006.
16. J. Fan and I. Gijbels. *Local Polynomial Modelling and Its Applications.* Chapman and Hall, London, 1996.
17. Jianqing Fan and Wenyang Zhang. Simultaneous confidence bands and hypothesis testing in varying-coefficient models. *Scand. J. Statist.*, 27(4):715–731, 2000.
18. H. T. Zhu, R. Z. Li, and L. L. Kong. Multivariate varying coefficient models for functional responses. Technical report, University of North Carolina at Chapel Hill, 2010.
19. S. Joshi, B. Davis, M. Jomier, and G. Gerig. Unbiased diffeomorphic atlas construction for computational anatomy. *Neuroimage*, 23:S151–S160, 2004.